Spectrometric Performances of CdTe and CdZnTe Semiconductor Detector Arrays at High X-ray Flux

A. Brambilla, C. Boudou, P. Ouvrier-Buffet, F. Mougel, G. Gonon, J. Rinkel, L. Verger

Abstract– **The development of a novel energy resolved fast X-ray imaging detector is reported. The device is based on pixellated cadmium telluride (CdTe) and cadmium zinc telluride (CdZnTe) detectors coupled to a custom designed 16-channel fast spectroscopy front-end electronic circuit. For each channel, a fast Analog to Digital Converter (ADC) continuously digitizes the signal from the detector pixel. A FPGA controls the acquisition and constructs the spectra on 256 energy bins for each channel.**

In this study, we measured the spectrometric performances with monochromatic X-rays from a synchrotron source at the European Synchrotron Radiation Facility (ESRF). We were able to acquire high-resolution pulse spectra for different X-ray energies and fluxes ranging from 10^5 to $2\ 10^7$ photons.mm^{-2}.s^{-1}. An energy resolution of 15% at 50 keV (7.5 keV FWHM) was obtained at 10^7 photons.mm^{-2}.s^{-1}. Additionally, first X-ray images in counting mode obtained with a 16-channels linear detector module are shown.

I. Introduction

There is a growing interest for high flux X-ray imaging detectors with energy discrimination or spectroscopy capabilities. Detectors made of compound semiconductors such as CdTe and CdZnTe have demonstrated outstanding performances for X and gamma ray spectrometry with room temperature operation [1].

Recently, energy sensitive CdTe and CdZnTe detectors for fast digital X-ray imaging have emerged [2-5]. They combine a fast read-out electronic circuit to provide high count rate capabilities and a coarse energy resolution obtained with a finite number of discriminators/counters for each detector channel.

LETI has been developing a novel fast read-out electronic capable to perform high-resolution spectrometry measurements at count rates above 10^7 counts/s. For each pixel, the signal is continuously digitized by a 100 MHz Analog to Digital Converter (ADC) and a FPGA controls the acquisition and reconstructs the energy spectra on 256 bins for each channel.

The read-out electronic was coupled to CdTe and CdZnTe pixel detectors and the spectrometric performances were characterized. A preliminary version of the detector with one single read-out channel was developed and tested under high flux monochromatic X-rays from a synchrotron source at the Euorpean Synchrotron Radiation Facility (ESRF). The measurements provided an extensive study of the performances in terms of energy resolution, efficiency and linearity of the detectors for X-rays at fluxes up to $2\ 10^7$ photons.mm^{-1}.s^{-1}.

First images under X-rays were obtained with a 16 channels detector module. The read-out circuit of this new device is in every way identical to the architecture of the prototype. It was coupled to a CdZnTe linear array pixel detector.

II. Detectors

A. Electronic read-out circuit

A new specific fast spectrometric readout electronics has been developed with commercial discrete components. The charges induced by X-rays interacting in the detector are amplified by a fast charge sensitive preamplifier and a shaping amplifier with a very short peaking time of typically 100 ns. A 100 MHz 12 bits ADC then continuously digitalizes the signal. A FPGA controls the acquisition and reconstructs the energy spectra on 256 energy bins. The spectra can be acquired in real time with an acquisition time ranging from as low as 3 ms. This novel architecture takes advantage from the FPGA which allows to implement advanced treatment on the digitized signal, such as baseline restoration or pile-up rejection.

B. Detector material

A 4x4 pixels CdTe detectors array has been purchased from ACRORAD (Japan). The pixel pitch is 800 µm and the detector thickness is 3 mm to ensure a good stopping power for X-rays up to 150 kV.

Manuscript received November 4, 2009.

A Brambilla, P. Ouvrier Buffet, F. Mougel, G. Gonon, J. Rinkel, and L. Verger are with CEA-LETI-MINATEC, Recherche Technologique, 17 rue de martyrs, 38054 Grenoble Cedex 09, France (e-mail: andrea.brambilla@cea.fr)

C. Boudou is with Thales Electron Devices, X-Ray Imaging Solutions, BP n° 122, 38346 Moirans Cedex, France

A 16 pixels CdZnTe linear array detector was purchased from eV-Products (USA). As for CdTe, the detector thickness is 3 mm, but the pixel area is 2.5 mm x 0.8 mm.

The detector geometry takes advantage of the small pixel effect [6]. It is now well established that the small pixel effect improves the spectrometric performances of CdTe and CdZnTe detectors: the most significant part of the signal is induced close to the collecting anode. The response of the detector is insensitive to incomplete collection of holes. Another advantage is a rise time by far faster than the complete transit time of electrons.

Note that CdZnTe and CdTe detectors do not have the same pixel geometry and special care must be taken when comparing the performances of the two detector materials, as the small pixel effect is different in each of the two detector materials.

III. Energy Resolution Measurements at ESRF

A. Experimental configuration

The ESRF was operating a 7/8+1 filling mode [6] yielding a maximal current of 202 mA: 7/8 of the storage ring (844.4 m) is filled with 868 bunches equally spaced by 2.83 ns and a single bunch is centered in the remaining 1/8 (Fig. 1). The temporal bunch width does not exceed few tens of ps. The electron circulation period is 2.8 µs and beam lifetime is about 55 h. It is obvious that our detector cannot resolve photons radiated from the same bunch. Also, photons generated from a series of successive bunches that does not exceed the detector dead time cannot be resolved. Considering the settings we worked with (see next paragraph), systematic coincidences, i.e. multiple photons originating from a single bunch, were very unlikely to occur.

We carried on experiments at the ID17 beamline whose instrumentation is described elsewhere [7]. Energy tuning is performed through a double Si monochromator and we operated measurement at 50 keV and 80 keV. Higher harmonics contribution are negligible.

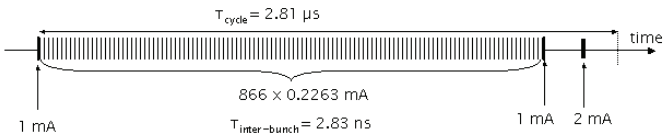

Fig. 1. Temporal description of a beam cycle for the 7/8+1 mode at the ESRF.

The beam was adjusted to cover the pixel area by a set of two parallel tungsten slits. Inserting blocs of PMMA (from 8 cm to 31.5 cm) into the beam allowed large variations of beam intensity. The incident flux was monitored through a HP-Ge detector functioning in integration mode. Also, the beam footprint at the CdTe/CdZnTe detector level was assessed by surface measurement onto a radiosensitive film. The global uncertainty on incident photon rate reaches 20% due to poor precision on film measurements.

B. Spectrometric performances

Fig. 2 shows sprectra from both detector types at 50 keV and 80 keV, acquired with a relatively low primary photon flux. Energy resolution and relative peak intensity are reported in Table 1. The energy resolution is derived from a Gaussian fit of the main peak. The relative peak intensity is the ratio of the counts that fall in the peak (within 4σ) divided by the total number of counts. The low pulse-height tail of the spectra is attributed to charge loss and charge sharing effects. Many physical phenomena can lead to the amplitude loss due to charge sharing effects: escape peaks from Cd and Te (K_α and K_β absorption edges) are visible within a single broad peak situated about 25 keV before the main peaks. Lateral expansion of the charge cloud due to Coulomb repulsion and diffusion of the photogenerated carrier can be involved. Also, incomplete charge collection arises from X-rays absorbed close to the collecting pixel, though is effect is greatly reduced by the small pixel effect [8].

At relatively low flux (Fig. 2), photon pile-up is negligible (more than 2 order of magnitude lower). At higher flux (see Fig. 3), photon pile-up occurs and peaks for 2 coincidence photons appear at 100 keV and 160 keV respectively for the 50 keV and 80 keV beams. Moreover, an extensive background signal is visible after the main peaks. This can be explained by partial energy pile-up from successive photons [9]. Also, high counts are visible at the end of spectrum: they represent all higher amplitude pulses from multiple coincidences that can not fit into the 256 bins. Note that the end of spectrum is not the same for both types of sensor because channel gain is slightly different.

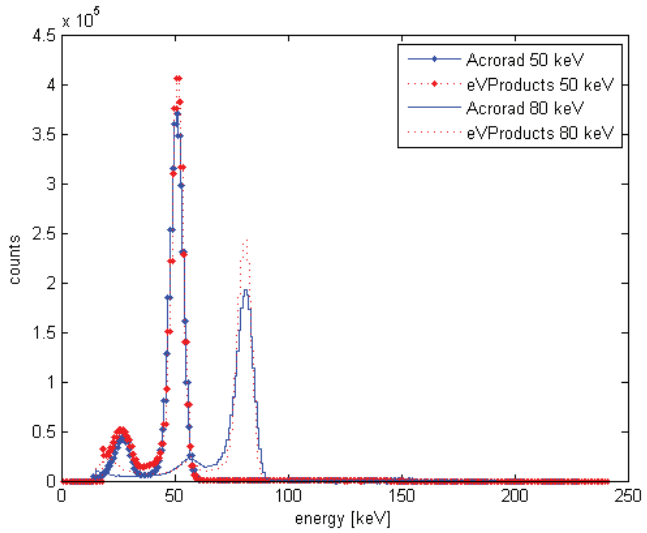

Fig. 2. Energy spectra obtained from 50 keV and 80 keV monochromatic beams under an incident flux of about 2 10^5 ph.mm^{-2}.s^{-1}.

TABLE. 1. RESOLUTION AND PEAK EFFICIENCY DETERMINED AT LOW COUNT-RATE (ABOUT 2 10^5 PH.MM^{-2}.S^{-1})

	Acrorad		eV-Products	
	50 keV	80 keV	50 keV	80 keV
Energy resolution (FWHM)	14.4 % (7.2 keV)	11.1 % (8.9 keV)	12.2 % (6.1 keV)	9.3 % (7.4 keV)
Peak efficiency (within 4σ)	85 %	78 %	79 %	74 %

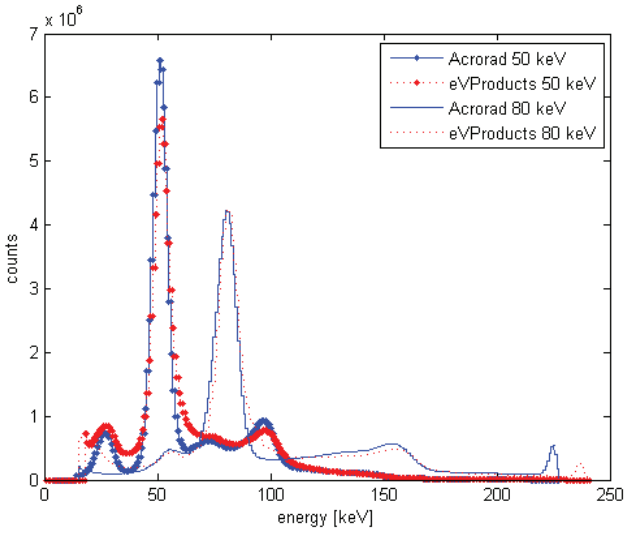

Fig. 3. Energy spectra obtained from 50 keV and 80 keV monochromatic beams under an incident flux of about 1 10^7 ph.mm^{-2}.s^{-1}

It is interesting to observe that at low flux, the energy resolution is better in the CdZnTe spectrum. However the peaks from CdZnTe broaden more noticeably than in CdTe spectra when incident photon rate is high. Plots of the full width at half maximum (FWHM) as a function of the X-ray primary flux at 80 keV display this trend clearly (Fig. 4). The energy resolution is increasing with increasing incident flux. For a primary photon flux of about 1 10^7mm^{-2}.s^{-1}, the resolution is close to 15% (7.5 keV) at 50 keV for both CdTe and CdZnTe detectors. Energy resolution measurement is favorable in the experiment configuration since charge sharing is negligible (the beam is sized to the pixel area).

The resolution of a detector at high count rate can be measured only from an intense monoenergetic X-ray source from a synchrotron. For comparison, Baümer et al. [10] extracted a 23 % energy resolution at a maximal incident rate of about 2 10^6 mm^{-2}.s^{-1} for 60 keV X-rays from a synchrotron radiation experiment with a CdZnTe sensor mounted on a NEXIS detection system. They obtained this result by scanning the discriminator thresholds over the range of relevant peak amplitudes. The lower energy resolution at high counting rate is mainly explained by the relatively high pulse length (350 ns) of the NEXIS system, limiting the performances at very high flux. Also the detector geometry, with pixel pitch of 1 mm and a detector thickness of 3 mm could be slightly less favorable to spectrometry.

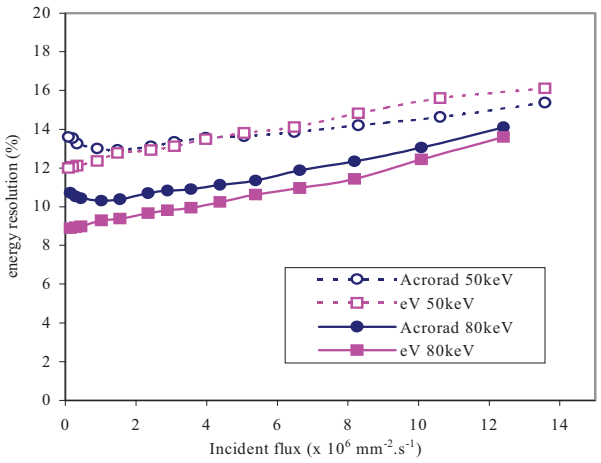

Fig. 4. Plot of energy resolution (FWHM) versus incoming flux from monoenergetic photon beam.

On Fig. 5, count rate is plotted versus the incident photon rate at 80 keV. A global count rate is obtained by summing all of the 256 energy bins. The detector response is fairly linear for count-rates up to 2 10^6 counts.s^{-1} and is monotonically increasing over the whole measured range of fluxes, reaching cont rates above 2 10^7 counts.s^{-1}. We applied a non-paralyzable detector model to fit the data with the measured incident photon rate despite the synchronous nature of the SR. Exact function expression is non trivial for a beam structure as the 7/8+1 mode and would required further investigation via Monte-Carlo simulation [11]. Values of detector dead time were derived from the fits: 109 ns for the Acrorad sensor and 114 ns for the eV-Products sensor. Saturation seems to occur above 6 10^6 counts.s^{-1} for an incident flux higher than 2 10^7 mm^{-2}.s^{-1} Similar results in terms of counting performance have been obtained with other imaging detector systems [4]. However, to our knowledge none provide a fully resolved energy spectrum over 256 bins at such fluxes.

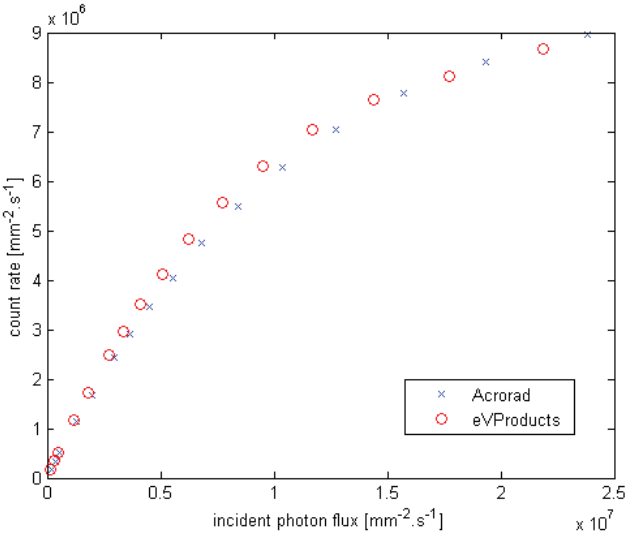

Fig. 5. Plot of count rate versus incident flux from a 80 keV monochromatic beam.

IV. IMAGING WITH THE 16-CHANNEL MODULE

A. 16-channel detector module

The detection module includes 16 channels in every way identical to the architecture of single channel reading electronic circuit prototype. One FPGA is used to control the acquisition and build the spectra for the 16 detector channels.

The read-out circuit was coupled to the CdZnTe linear array pixel detector from eV-Products, which was previously used for the spectrometric measurements with monochromatic X-rays.

B. Spectrometric measurements with radioactive sources

We have performed measurements with a ^{57}Co (122 keV and 136 keV peaks) gamma-ray source in order to characterize the spectrometric performances of the CdZnTe detector coupled with the 16 channels electronic read-out circuit. Fig. 6 shows spectra from the 16 pixels. Spectra are quite alike with slight variations of the peak position that are due to the gain differences between channels. The energy resolution is 5.5 % (6.7 keV FWHM) for the 122 keV peak and is almost independent from the channel number**.** The electronic noise, measured from pulses injected from an external generator, is 5.1 keV (FWHM). These values are comparable to those obtained with the single channel prototype with monochromatic radiations from a synchrotron source. However, the low energy tail is much more important in these measurment with a gamma source. The low energy tail is due to small pulses induced by photons interacting on the neighboring pixel and is a consequence of the signal formation in small pixel detectors. This effect is a consequence of the small pixel effect and has been described elsewhere in detail (see for instance [12]): when electrons generated close to the common cathode drift toward the collecting pixel, a small positive current is induced on the neighboring pixels. In the absence of trapping, the induced current increases abruptly when the electrons reach the collecting pixel. In the meantime a negative current is induced on the neighboring pixel that will compensate the initial positive current. However, the initial current might be sufficient to trigger the event and a low energy pulse is counted on one or more pixels. This effect is responsible for the lower part of the pulse-height spectra with an important number of pulses with amplitude slightly above the detection threshold. This effect, which was not observed on the measurements performed with a highly collimated beam at ESRF shows the importance of the pixel design in order to optimize the small pixel effect.

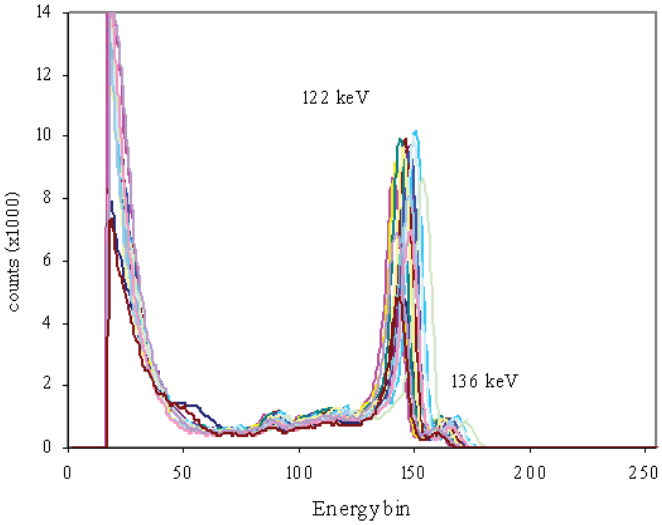

Fig. 6. Energy spectra obtained through the CdZnTe 16 pixels linear detector array with a ^{57}Co source.

C. Imaging performances

In order to validate imaging performance of the 16 pixel array detector, we placed a hand phantom onto a 2 moving axis test bench. Figure 7 shows the acquisition performed with the eV-Products sensor, collimated with a tungsten slit of 800 µm width and with following source parameters: 50 kV, 0.9 mA, 3 mm Al filtration, corresponding to an incident flux of 2 10^5 photons.mm^{-2}.s^{-1}.

Even without gain correction, the hand transmission image is clearly identifiable. The horizontal lines are due to the different sensitivities between pixels. In particular, the two edge pixels are slightly smaller to allow tilling of detectors with preservation of the pixel pitch. It is noticeable that a simple gain correction is enough to obtain a good image quality. This result is obtained because the image was acquired at low count rate. At higher count rates it may be necessary to include a correction of non-linearity that takes into account the reduced sensitivity due to the dead time of the detector [13].

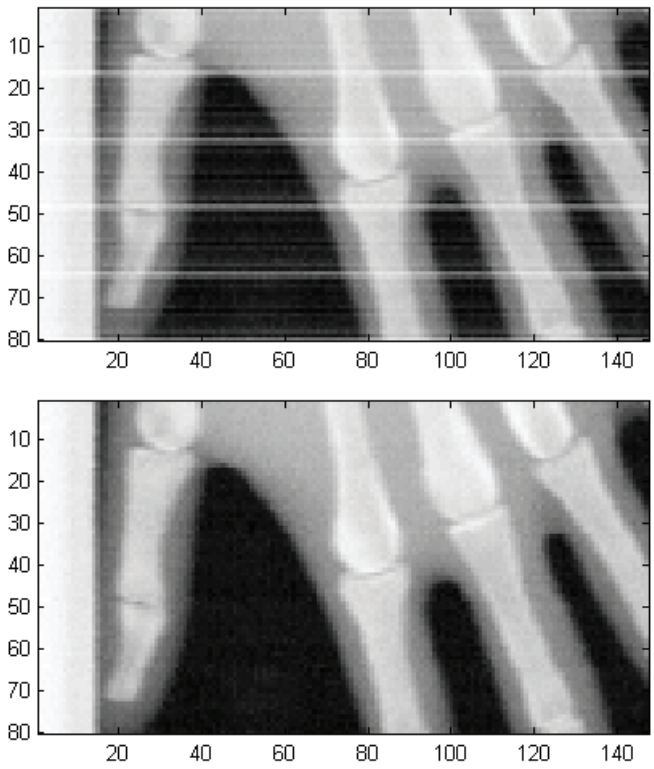

Fig. 7. Image of a hand phantom acquired by scanning the phantom above the 16 pixels linear array. Top: raw acquisition, and bottom; acquisition corrected from gain. The numbers on the axis indicate the number of pixels (pixel size: 800 µm x 800 µm).

V. Conclusion

We have presented an extensive study of the spectrometric performances of a innovative energy resolved detector for X-ray imaging. Our detector exhibits a very low dead time while providing a full energy spectrum in a single measurement over many pixels. The measurements performed with high flux monochromatic X-rays from a synchrotron source shows that excellent spectrometric performances are achieved at fluxes up to $2\,10^7$ photons.mm^{-2}.s^{-1}. Energy resolution of 15% at (7.5 keV FWHM) is achieved at 10^7 photons.mm^{-1}.s^{-1} for 50 keV photons.

Acknowledgment

We are indebted to the European synchrotron Radiation Facility (Grenoble, France) for providing beamtime. We thank Alberto Bravin and Herwig Requardt for assistance in preparing the experiment and for technical support. CB thanks Laurent Hardy for discussions about the ESRF operation mode.

References

[1] L. Verger, E. Gros d'Aillon, O. Monnet, G. Montémont, and B. Pelliciari, "New trends in gamma-ray imaging with CdZnTe/CdTe at CEA-Leti", *Nuclear Instruments and Methods in Physics Research Section A: Accelerators, Spectrometers, Detectors and Associated Equipment*, 2007. **571**(1-2): p. 33-43.

[2] V. B. Cajipe, R. F. Calderwood, M. Clajus, S. Hayakawa, R. Jayaraman, T. O. Tumer, B. Grattan, O. Yossifor, R. Nova, and R. D, "Multi-energy X-ray imaging with linear CZT pixel arrays and integrated electronics", *Nuclear Science Symposium Conference Record, 2004 IEEE*, 2004. **7**.

[3] Hamamatsu. *64ch CdTe Radiation Line Sensor*. 2009 [cited Oct. 2009]. Available from: http://jp.hamamatsu.com/products/x-ray/pd451/C10413/index_en.html.

[4] J. S. Iwanczyk, E. Nygard, O. Meirav, J. Arenson, W. C. Barber, N. E. Hartsough, N. Malakhov, and J. C. Wessel, "Photon counting energy dispersive detector arrays for x-ray imaging", *IEEE Transactions on Nuclear Science*, 2009. **56**(3): p. 535-542.

[5] S. Mikkelsen, D. Meier, G. Maehlum, P. Oya, B. Sundal, and J. Talebi. "An ASIC for multi-energy x-ray counting". in *IEEE Nuclear Science Symposium Conference Record*, 2008, Desden, Germany.

[6] ESRF. *Operating Modes - ESRF*. 2007 [cited 2008-07-11]. Available from: http://www.esrf.eu/Accelerators/Operation/Modes.

[7] H. Elleaume, A. M. Charvet, P. Berkvens, G. Berruyer, T. Brochard, Y. Dabin, M. C. Dominguez, A. Draperi, S. Fiedler, and G. Goujon, "Instrumentation of the ESRF medical imaging facility", *Nuclear Instruments and Methods in Physics Research A*, 1999. **428**: p. 513-527.

[8] H. H. Barrett, J. D. Eskin, and H. B. Barber, "Charge Transport in Arrays of Semiconductor Gamma-Ray Detectors", *Physical Review Letters*, 1995. **75**(1): p. 156-159.

[9] R. Bates, G. Derbyshire, W. J. F. Gannon, G. Iles, B. Lowe, K. Mathieson, M. S. Passmore, M. Prydderch, P. Seller, and K. Smith, "Performance of an energy resolving X-ray pixel detector", *Nuclear Instruments and Methods in Physics Research Section A: Accelerators, Spectrometers, Detectors and Associated Equipment*, 2002. **477**(1): p. 161-165.

[10] C. Bäumer, G. Martens, B. Menser, E. Roessl, J. P. Schlomka, R. Steadman, and G. Zeitler, "Testing an Energy-Dispersive Counting-Mode Detector With Hard X-Rays From a Synchrotron Source", *IEEE Transactions On Nuclear Science* 2008. **55**(3): p. 1785.

[11] J. E. Bateman, "The effect of beam time structure on counting detectors in SRS experiments", *Journal of Synchrotron Radiation*, 2000. **7**(5): p. 307-312.

[12] S. E. Anderson, B. Donmez, and Z. He. "Sub-pixel position resolution in pixelated semiconductor detectors". in *IEEE Nuclear Science Symposium Conference Record*, 2007.

[13] C. Szeles, S. A. Soldner, S. Vydrin, J. Graves, and D. S. Bale, "Ultra High Flux 2-D CdZnTe Monolithic Detector Arrays for X-Ray Imaging Applications", *IEEE Transactions on Nuclear Science*, 2007. **54**(4 Part 3): p. 1350-1358.